Barrier Coverage in Bistatic Radar Sensor Networks: Cassini Oval Sensing and Optimal Placement

Xiaowen Gong
Arizona State University
Tempe, AZ 85287, USA
xgong9@asu.edu

Junshan Zhang
Arizona State University
Tempe, AZ 85287, USA
junshan.zhang@asu.edu

Douglas Cochran
Arizona State University
Tempe, AZ 85287, USA
cochran@asu.edu

Kai Xing
University of Science and Technology of China
Hefei, Anhui 230027, China
kxing@ustc.edu.cn

ABSTRACT

By taking advantage of active sensing using radio waves, *radar* sensors can offer several advantages over passive sensors. Although much recent attention has been given to multistatic and MIMO radar concepts, little has been paid to understanding the performance of radar networks (i.e., multiple individual radars working in concert). In this context, we study the optimal placement of a *bistatic radar* (BR) sensor network for barrier coverage. The coverage problem in a bistatic radar network (BRN) is challenging because: 1) in contrast to the disk sensing model of a traditional passive sensor, the sensing region of a BR depends on the locations of both the BR transmitter and receiver, and is characterized by a *Cassini oval*; 2) since a BR transmitter (or receiver) can potentially form multiple BRs with different BR transmitters (or receivers, respectively), the sensing regions of different BRs are coupled, making the coverage of a BRN highly non-trivial.

This paper considers the problem of deploying a network of BRs in a region for maximizing the *worst-case intrusion detectability*, which amounts to minimizing the *vulnerability* of a *barrier*. We show that the *shortest barrier*-based placement is optimal if the shortest barrier is also the shortest line segment connecting the region's two boundaries. Based on this observation, we study the optimal placement of the BRs on a line segment for minimizing its vulnerability, which is a non-convex optimization problem. By exploiting some specific structural properties pertaining to the problem (particularly an important structure of detectability), we find the optimal *placement order* and the optimal *placement spacing* of the BR nodes, both of which exhibit elegant *balanced* structures. Our findings give valuable insight for the placement of BRs for barrier coverage. To our best knowledge, this is the first work to explore the coverage of a network of BRs.

MobiHoc'13, July 29–August 1, 2013, Bangalore, India.

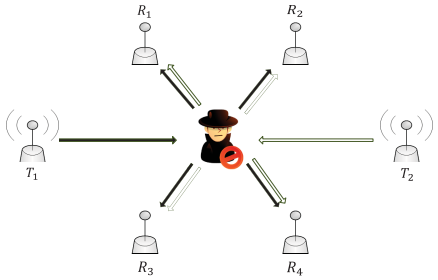

Figure 1: A bistatic radar network consisting of 2 radar transmitters T_1, T_2 and 4 radar receivers R_1, R_2, R_3, R_4. Each transmitter-receiver pair operates as a bistatic radar.

Categories and Subject Descriptors

C.2.1 [**Computer-Communication Networks**]: Network Architecture and Design—*Network Topology*

Keywords

Barrier Coverage, Bistatic Radar Sensor Network, Optimal Placement, Worst-case Intrusion

1. INTRODUCTION

Wireless sensor networks have received tremendous attention over the past decade. Typically, it is assumed that a sensor network is composed of *passive sensors* (e.g., thermal, acoustics, optic sensors) which detect radiation that is emitted or reflected by an object. In contrast, an active *radar* (RAdio Detection And Ranging) purposefully emits radio waves with the objective of collecting echoes. The ability to design the structure and power of the transmitted radio signal imbues active radars with performance advantages over passive sensors in many application scenarios, though this is typically at the expense of additional system complexity.

Thanks to recent technological advances, radars are becoming less expensive and more compact, making it feasible to deploy a network of radars working in concert. Indeed, the application scale and scope of networked radar sensors[1] are

[1]For brevity, we may use "radar" and "radar sensor" interchangeably.

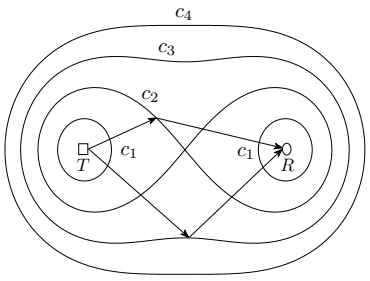

Figure 2: Bistatic radar SNR contours as Cassini ovals with foci at BR transmitter T and receiver R for distance products: $c_1 < c_2 < c_3 < c_4$.

expected to expand significantly. Due to radars' advantages over traditional passive sensors, radar networks have great potential for many applications, such as border security [1] and traffic monitoring [2]. Nevertheless, to fully exploit this potential, radar networks should be judiciously designed.

Coverage, which defines how well the object of interest is monitored, is a critical performance metric for sensor networks. *Barrier coverage* has recently emerged as an efficient coverage strategy for numerous sensor network applications centered around *intruder detection*, such as border monitoring and drug interdiction, and has drawn a surge of research interest [3–6]. Despite tremendous research progress on coverage problems for sensor networks [7], those pertaining to radar sensors remain largely unexplored, and this is the main subject of this study.

In this paper, we consider the problem of deploying a network of bistatic radars (BRs) for intrusion detection. Due to the flexibility to deploy the radar transmitter and receiver separately, a BR is more favorable than a monostatic radar (MR) for coverage. Our goal is to *build a fundamental understanding of a bistatic radar network (BRN) for coverage.* In particular, a central question we ask here is: *Where should the BRs be placed to achieve the optimal coverage quality?*

The coverage problem of a BRN is dramatically different and more challenging than that of a network of traditional passive sensors, because 1) departing from the disk sensing model of a passive sensor, the sensing region of a BR depends on the locations of both transmitter and receiver, and is characterized by a Cassini oval. Formally, a Cassini oval is a locus of points for which the distances to two fixed points (foci) have a constant product (as illustrated in Figure 2); 2) the sensing regions of different BRs are coupled with each other, since each BR transmitter[2] (or receiver) can potentially pair with different BR receivers (or transmitters, respectively) to form multiple BRs such that its location would impact multiple BRs.

We summary the main contributions of this paper as follows.

- We consider the problem of deploying a network of BRs in a region for maximizing the *worst-case intrusion detectability*, which is equivalent to minimizing the *vulnerability* of a *barrier*. We show that the *shortest barrier*-based placement is not optimal in general, and it is optimal if the shortest barrier is also the shortest line segment connecting the region's two boundaries.
- We focus on characterizing the optimal placement of the BRs on a line barrier for minimizing its vulnerability, *which is a highly non-trivial optimization problem due to its non-convexity.* To tackle the challenges herein, we reformulate the problem as finding the optimal *placement order* with the optimal *placement spacing* of the BR nodes. Based on an important structure of detectability, we characterize *balanced* placement spacing and show that it is optimal. Based on the optimal placement spacing, we then characterize the optimal placement orders, which also present balanced structures. These findings provide valuable insight for the placement of BRs for barrier coverage.

Although it is somewhat idealized, the Cassini oval sensing model (see SNR equation (1)) used in this paper can capture the essential feature of a BR, compared to a passive sensor or MR. Furthermore, the coverage problem of a BRN corresponding to the Cassini oval sensing model gives rise to significant technical difficulties (as will be seen later). Needless to say, future work is needed to generalize this study to more complex and realistic situations. In short, we believe that this study will open a new door to explore radar sensor networks.

The rest of this paper is organized as follows. Section 2 introduces the model of our work and the problem definition. In Section 3, we investigate our problem based on the barrier coverage strategy. We study the optimal placement of BRs on a line barrier in Section 4. Section 5 provides numerical results and Section 6 reviews the related works. Section 7 concludes this paper and discusses future works.

2. MODEL AND PROBLEM DEFINITION

In this section, we first describe the model of our work, including bistatic radar network and network coverage, and then introduce the problem definition.

2.1 Bistatic Radar Network

The radar transmitter and receiver are placed at different locations for a BR, whereas they are co-located for a MR. Intuitively, a BR can achieve enhanced coverage by appropriate placement of the transmitter and receiver, such that an object is more likely to be physically closer to either a transmitter or receiver, and thus attains a high signal-to-noise ratio (SNR). This advantage of BR will be illustrated by a concrete example in Section 3.

One important metric of a BR's capability for target detection is its received SNR: the strength of the received radar signal indicates whether the target is present. Let $\|AB\|$ and $\overline{AB}$ denote the (Euclidean) distance and the line segment between two points A and B, respectively. For convenience, we also use T_i or R_j to denote the location (point) of a BR transmitter node T_i or receiver node R_j, respectively. For a BR $T_i - R_j$, the received SNR from the target at a point X is given by [8]:

$$\text{SNR} = \frac{K}{\|T_iX\|^2\|R_jX\|^2} \tag{1}$$

where K denotes a *bistatic radar constant* that reflects physical characteristics of the BR, such as transmit power, *radar*

[2]For brevity, we may say "transmitter" and "receiver" instead of "BR transmitter" and "BR receiver", respectively.

cross section[3], transmitter and receiver antenna power gains. The SNR contours of a BR are characterized by the Cassini ovals with foci at the transmitter and receiver.

In a network of BRs, we assume that all transmitters operate on orthogonal radio resources (e.g., different frequencies or time slots, orthogonal waveforms) to avoid interferences at receivers. While multiple receivers can pair with the same transmitter to form multiple BRs, one receiver can also pair with multiple transmitters (e.g., by tuning to different transmitters in different time slots periodically). Typically, a BRN has more receivers than transmitters, mainly because that a transmitter incurs higher cost than a receiver (e.g., since signal transmission consumes much more energy than other sensor activities including signal reception and processing). In addition, the number of transmitters can also be limited by the available radio resources (e.g., the number of different frequencies).

We consider the deployment of a BRN consisting of M transmitters $T_i \in \mathcal{T}$, $i \in \mathcal{M} \triangleq \{1, \cdots, M\}$ and N receivers $R_j \in \mathcal{R}$, $j \in \mathcal{N} \triangleq \{1, \cdots, N\}$ where $M \leq N$. For ease of exposition, we assume that transmitters and receivers, respectively, have homogeneous physical characteristics such that all BRs have the same bistatic radar constant. We also assume that a receiver can potentially pair with all transmitters to form multiple BRs. However, our results in Section 4 will show that it suffices for a receiver to pair with *at most two* transmitters. We further assume that transmitted and reflected radar signals are *omni-directional*[4].

2.2 Network Coverage

The BRN is deployed in a 2D geographical *region of interest* F for detecting an intruder traversing through the region. The region F is defined by an entrance side, a destination side, a left boundary F_l, and a right boundary F_r (as illustrated in Figure 3). The intruder can choose any *intrusion path* P in region F connecting the entrance to the destination.

The existing studies on sensor network coverage [9–11] have used the distance from a point to its *closest* sensor to measure the coverage of that point (also known as the *closest sensor observability*). In the same spirit, we measure the coverage of a point by the *highest* SNR received by all BRs when the target is present at that point. Considering (1), we have the following definition.

DEFINITION 1 (**Detectability**). *The detectability*[5] $I(X)$ *of a point* X *is the minimum distance product from* X *to all BRs:*

$$I(X) \triangleq \min_{T_i \in \mathcal{T}, R_j \in \mathcal{R}} \|T_i X\| \|R_j X\|. \quad (2)$$

In other words, the detectability of a point is determined by the point's *closest BR* consisting of its closest transmitter and closest receiver. As in [9–11], we use the *worst-case intrusion* to quantify the coverage of the intruder.

[3]Radar cross section measures the amount of radar signal energy reflected by an object depending on its physical characteristics (e.g., shape, material).

[4]The propagation direction of the reflected radar signal depends on the object's physical characteristics (e.g., shape, material), and is not omni-directional in general.

[5]With a little abuse of notation, we use $I(X)$ to denote the detectability of X, but X's detectability changes inversely with the value of $I(X)$.

DEFINITION 2 (**Worst-case Intrusion [9]**).*The worst-case intrusion path* P^* *is the intrusion path with the minimum detectability:*

$$P^* \triangleq arg \max_{P \in \mathcal{P}} D(P) \quad (3)$$

where $\mathcal{P}$ *is the set of all possible intrusion paths, and the detectability* $D(P)$ *of an intrusion path* P *is the maximum detectability of all points in* P*:*

$$D(P) \triangleq \min_{X \in P} I(X). \quad (4)$$

2.3 Problem Definition

We are interested in finding the optimal placement of the BRN (i.e., optimal locations of M transmitters and N receivers) in region F for maximizing the worst-case intrusion detectability:

$$\underset{T_i \in F, R_j \in F}{\text{minimize}} \quad D(P^*). \quad (5)$$

Based on the notion of worst-case intrusion, problem (5) is of great interest for the intruder detection problem. In particular, solving problem (5) allows us to answer an important question: How many transmitters and receivers are needed and where do we place them for providing the required coverage such that *at least one* BR will receive an SNR above some predefined threshold, regardless of the intruder's path?

It is worth noting that problem (5) is difficult to solve in general (even for a sensor network under the disk sensing model). This is because 1) the shape of region F can be arbitrary and 2) the feasible solution space, which includes any placement in region F, is large. In the next section, we will investigate problem (5) based on the strategy of barrier coverage.

3. PLACEMENT FOR BARRIER COVERAGE

In this section, we consider problem (5) by placing the BRs for barrier coverage. As in [3–6], a *barrier* is defined as a curve lying in region F such that *any* intrusion path intersects with the curve. We next define the coverage metric of a barrier.

DEFINITION 3 (**Vulnerability**). *The vulnerability* $V(U)$ *of a barrier* U *is the minimum detectability of all points in* U*:*

$$V(U) \triangleq \max_{X \in U} I(X). \quad (6)$$

The rationale of using such a coverage metric is that, since a barrier intersects with any possible intrusion path, the vulnerability of a barrier serves as an *upper bound* on the worst-case intrusion detectability. This bound becomes *tight* when all barriers are considered:

$$D(P^*) = \min_{U \in \mathcal{U}} V(U) \quad (7)$$

where $\mathcal{U}$ is the set of all barriers.

Using (7), problem (5) boils down to finding the optimal barrier that has the minimum *achievable vulnerability* $V^*(U)$:

$$\underset{U \in \mathcal{U}}{\text{minimize}} \quad V^*(U), \quad (8)$$

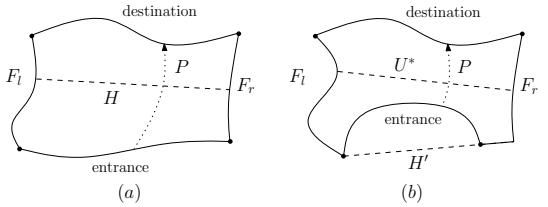

Figure 3: (a) H is the shortcut barrier; (b) H' is the shortest line segment connecting F_l and F_r but not a barrier, so the shortcut barrier does not exist; the shortest barrier U^* (also a line barrier) is not the shortcut barrier.

where $V^*(U)$ is the vulnerability of U under the optimal placement of the BRs in region F for minimizing U's vulnerability, i.e., the optimal value of the following problem:

$$\underset{T_i \in F, R_j \in F}{\text{minimize}} \quad V(U). \tag{9}$$

For problem (8), it seems plausible to select the *shortest barrier* U^*, which is the barrier (possibly multiple) with the minimum length. However, this strategy is not optimal in general because $V^*(U^*)$ is not necessarily lower than $V^*(U)$ for a barrier U with a *larger* length than U^*. We give a simple counterexample as illustrated in Figure 4. For a line barrier[6] $\overline{AB}$ in Figure 4(a), one can easily figure out that the optimal placement of a BR $T-R$ is to set $\|AT\| = \|RB\| = \sqrt{2}-1$ such that $V^*(\overline{AB}) = \|AT\|\|AR\| = 1$. For a barrier $\widetilde{CF}$[7] consisting of $\overline{CD}$, $\overline{DE}$, $\overline{EF}$ in Figure 4(b), which has a larger length than $\overline{AB}$, we have $V^*(\widetilde{CF}) \le V(\widetilde{CF}) = \|TE\|\|ER\| = \sqrt{5}/4 < 1$ where T and R are placed at the midpoints of $\overline{CD}$ and $\overline{EF}$, respectively.

Before proceeding further, we use a simple example to illustrate the advantage of a BR over a MR for barrier coverage. If we place a MR (co-located transmitter and receiver) on $\overline{AB}$ in Figure 4(a) to minimize $V(\overline{AB})$, the optimal placement is clearly at the midpoint G of $\overline{AB}$ such that $V(\overline{AB}) = \|AG\|^2 = 2$, which is greater than $V^*(\overline{AB}) = 1$.

Although the shortest barrier-based placement is not optimal in general, it is optimal if the shortest barrier is also the *shortcut barrier*.

DEFINITION 4 (**Shortcut Barrier**). *The shortcut barrier exists and is the shortest barrier if and only if the shortest barrier is the shortest line segment connecting F_l and F_r (i.e., its length is the minimum distance between a point in F_l and a point in F_r).*

Although there must exist the shortest line segment connecting F_l and F_r, it does not necessarily lie in region F as a barrier (as illustrated in Figure 3(b)). The shortcut barrier exists for a large class of shapes of region F. For example, any convex region falls in this class. Worth noting is that if the shortest barrier is not the shortcut barrier, it can still be a line barrier (as illustrated in Figure 3(b)).

THEOREM 1. *If the shortcut barrier H exists, then it is the optimal barrier for problem* (8)*, indicating that it suffices to solve problem* (9) *for H.*

[6]We refer a barrier as a line barrier if it is a line segment.

[7]We use $\widetilde{PQ}$ and $\|\widetilde{PQ}\|$ to denote a curve with end points P and Q, and its length, respectively.

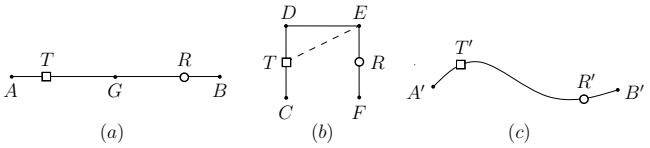

Figure 4: (a) $\|AB\| = 2\sqrt{2}$; (b) $\|CD\| = \|DE\| = \|EF\| = 1$, $\overline{CD} \perp \overline{DE}$, $\overline{EF} \perp \overline{DE}$; (c) $\|\widetilde{A'B'}\| = 2\sqrt{2}$.

We can show that the optimal placement for problem (9) for a line barrier is *on* that barrier. In view of the optimality of the shortcut barrier-based placement, in Section 4, we will focus on finding the optimal placement of the BRs on a line barrier for minimizing its vulnerability.

If the shortest barrier U^* is not the shortcut barrier, it can be an arbitrary curve and it is not necessarily the optimal barrier for problem (8). Furthermore, it is in general difficult to find the optimal placement for problem (9) for an arbitrary barrier (even for a sensor network under the disk sensing model). In this situation, we can take an *approximate* approach for U^* by applying the optimal placement for problem (9) for a line barrier (will be obtained in Section 4). Specifically, we can treat U^* as a line barrier $\overline{U^*}$ (if U^* is not) with the same length, and place the BR nodes on U^* according to the optimal placement for $\overline{U^*}$. An appealing property of this approach is that $V(U^*)$ under such placement must be *no greater than* $V^*(\overline{U^*})$, and hence $V^*(\overline{U^*})$ serves as an upper bound for the worst-case intrusion detectability $D(P^*)$. For example, as $\overline{AB}$ in Figure 4(a) has the same length with $\widetilde{A'B'}$ in Figure 4(c), we can apply the optimal placement of $\{T, R\}$ for minimizing $V(\overline{AB})$ to $\widetilde{A'B'}$ such that $\|\widetilde{A'T'}\| = \|AT\|$ and $\|\widetilde{T'B'}\| = \|TB\|$. Then we have that $V(\widetilde{A'B'})$ under $\{T', R'\}$ is no greater than $V^*(\overline{AB})$ under $\{T, R\}$. Since we can show that $V^*(U)$ for a line barrier U is increasing with U's length and U^* has the minimum length, applying the approximate approach to U^* can achieve the *minimum* upper bound $V^*(\overline{U^*})$ for $D(P^*)$ compared to applying it to other barriers.

4. OPTIMAL PLACEMENT ON A LINE BARRIER

In this section, we study the optimal placement of the BRs on a line barrier (line segment) H for minimizing its vulnerability $V(H)$.

4.1 Problem Reformulation

Let H_l and H_r be the end points of H and h be its length. Also let $t_i \triangleq \|H_l T_i\|$ and $r_j \triangleq \|H_l R_j\|$. Mathematically, the problem can be written as

$$\begin{aligned} \underset{t_i, r_j}{\text{minimize}} \quad & \max_{0 \le x \le h} \min_{i \in \mathcal{M}, j \in \mathcal{N}} |x - t_i||x - r_j| \\ \text{subject to} \quad & 0 \le t_i \le h, \forall i \in \mathcal{M} \\ & 0 \le r_j \le h, \forall j \in \mathcal{N} \end{aligned} \tag{10}$$

where $\min_{i \in \mathcal{M}, j \in \mathcal{N}} |x - t_i||x - r_j|$ represents the detectability of a point $X \in H$ with $\|H_l X\| = x$. Since we can show that problem (10) is *non-convex* in general, standard optimization methods would not work well here.

To gain more insight of problem (10), we reformulate it as follows. We first treat H_l and H_r as two (virtual) nodes

and ignore the constraint $\|H_lH_r\| = h$. Then we place H_l, H_r, and all the BR nodes on a horizontal line such that H_l and H_r are the *leftmost* and *rightmost* nodes, respectively.

DEFINITION 5 (**Placement Order and Spacing**). *A placement order ("order" for short)* $\mathbf{S}$ *is an order of all the nodes on the line from left to right:*

$$\mathbf{S} \triangleq (H_l, S_1, \cdots, S_J, H_r)$$

where $J \triangleq M + N$ *and* $(S_1, \cdots, S_J)$ *is a permutation of the BR nodes such that* $\|H_lH_l\| \leq \|H_lS_1\| \leq \cdots \leq \|H_lS_J\| \leq \|H_lH_r\|$. *The placement spacing ("spacing" for short)* $\mathbf{D_S}$ *of a placement order* $\mathbf{S}$ *consists of the distances between neighbor nodes in* $\mathbf{S}$*:*

$$\mathbf{D_S} \triangleq (\|H_lS_1\|, \cdots, \|S_JH_r\|).$$

A local placement order ("local order" for short) $(S_{i+1}, \cdots, S_{i+j})$ *is an order of some neighbor nodes in* $\mathbf{S}$*, and its placement spacing is*

$$\mathbf{D}_{(S_{i+1}\cdots,S_{i+j})} \triangleq (\|S_{i+1}S_{i+2}\|, \cdots, \|S_{i+j-1}S_{i+j}\|).$$

Any order $\mathbf{S}$, together with any spacing $\mathbf{D_S}$, correspond to some placement of the BRs on a line segment with length $\|H_lH_r\|$; conversely, any placement of the BRs on the line segment H has a corresponding order $\mathbf{S}$ with corresponding spacing $\mathbf{D_S}$ subject to $\|H_lH_r\| = h$. Therefore, problem (10) can be recast as

$$\begin{aligned} \underset{\mathbf{S},\mathbf{D_S}}{\text{minimize}} \quad & V(\overline{H_lH_r}) \\ \text{subject to} \quad & \|H_lH_r\| = h. \end{aligned} \tag{11}$$

For any order $\mathbf{S}$, we note that the vulnerability $V(\overline{H_lH_r})$ is *non-decreasing* as any distance in $\mathbf{D_S}$ increases. In light of this, we can formulate a related problem of problem (11) as

$$\begin{aligned} \underset{\mathbf{S},\mathbf{D_S}}{\text{maximize}} \quad & \|H_lH_r\| \\ \text{subject to} \quad & V(\overline{H_lH_r}) \leq c. \end{aligned} \tag{12}$$

Let l_c denote the optimal value of problem (12) under the constraint $V(\overline{H_lH_r}) \leq c$. We can verify that l_c is strictly increasing in c and, in particular, $l_c \to 0$ when $c \to 0$ and $l_c \to \infty$ when $c \to \infty$. Therefore, if we can solve problem (12) for any $c > 0$, we can also solve problem (11) by a *bisection search* described in Algorithm 1.

We make two general observations to be used later. First, since all BRs are homogeneous, swapping the locations of any pair of transmitters (or receivers, respectively) results in an equivalent placement. Second, transmitters and receivers are *reciprocal* in the sense that replacing all transmitters by receivers while replacing all receivers by transmitters results in an equivalent placement.

4.2 Optimal Placement Order and Spacing

In this subsection, we focus on characterizing the optimal order and the optimal spacing for problem (12). We outline the major steps as follows.

1) We identify an important structure of detectability on $\overline{H_lH_r}$ (Lemma 1), based on which we define *balanced spacing*.

Algorithm 1: Compute the optimal solution to problem (11)

input : the line barrier length h, tolerance ϵ
output: the optimal order $\mathbf{S}^*$, the optimal spacing $\mathbf{D}^*_{\mathbf{S}^*}$, the optimal value c^*

$c_1 \leftarrow 0$, $c_2 \leftarrow h^2$, $c \leftarrow \frac{c_1+c_2}{2}$;
repeat
  compute the optimal order $\mathbf{S}^*$ with the optimal spacing $\mathbf{D}_{\mathbf{S}^*}$ for problem (12) subject to $V(\overline{H_lH_r}) \leq c$;
  if $l_c > h + \epsilon$ **then**
    $c_2 \leftarrow c$; $c \leftarrow \frac{c_1+c_2}{2}$;
  end
  if $l_c < h - \epsilon$ **then**
    $c_1 \leftarrow c$; $c \leftarrow \frac{c_1+c_2}{2}$;
  end
until $|l_c - h| \leq \epsilon$;
return $\mathbf{S}^*$, $\mathbf{D}^*_{\mathbf{S}^*}$, $c^* \leftarrow c$;

2) We define *independent local orders*. Then we characterize the balanced spacing for an independent local order (Lemma 2) and show that it is optimal (Lemma 3).

3) We show that the optimal order consists of independent local orders with *disjoint* sets of spacing distances (Lemma 4), based on which we show that the balanced spacing is optimal for the optimal order (Theorem 2).

4) Based on the optimal spacing, we characterize the optimal orders (Theorem 3).

Let Y_{AB} denote the midpoint between two points A and B. We first show an important structure of detectability on $\overline{H_lH_r}$.

LEMMA 1. *For any order* $\mathbf{S}$ *with any spacing* $\mathbf{D_S}$*, the detectability on* $\overline{H_lH_r}$ *attains local maximums at the end nodes and at the midpoints of all pairs of neighbor nodes in* $(S_1, \cdots, S_J)$ *(as illustrated in Figure 5):*

$$\arg \max_{X \in \overline{H_lS_1}} I(X) = H_l, \quad \arg \max_{X \in \overline{S_JH_r}} I(X) = H_r$$
$$\arg \max_{X \in \overline{S_iS_{i+1}}} I(X) = Y_{S_iS_{i+1}}, \quad \forall i \in \{1, \cdots, J-1\}.$$

DEFINITION 6 (**Local Vulnerable Point**). *A local vulnerable point is a local maximum point of detectability on* $\overline{H_lH_r}$ *(described in Lemma 1), and a local vulnerable value is its detectability.*

By Lemma 1, it suffices to focus on the local vulnerable values for determining the vulnerability of $\overline{H_lH_r}$.

DEFINITION 7 (**Independent Local Order**). *A local order* $\mathbf{S}_i$ *is an independent local order if it exhibits one of the following orders of node types (*H_l*,* H_r*, transmitter type* T*, or receiver type* R*):*

$$(T, R^k, H_r), (R, T^k, H_r), (H_l, R^k, T), (H_l, T^k, R), k \geq 1;$$

$$(T, R^k, T), (R, T^k, R), k \geq 1; \quad (T, R), (R, T);$$

where we use T^k *or* R^k *to denote* k *consecutive* T *or* R*, respectively. The independent local zone* $Z_{\mathbf{S}_i}$ *of an independent local order* $\mathbf{S}_i$ *is the line segment between the two end nodes in* $\mathbf{S}_i$*, with its length denoted by* $L_{\mathbf{S}_i}$*.*

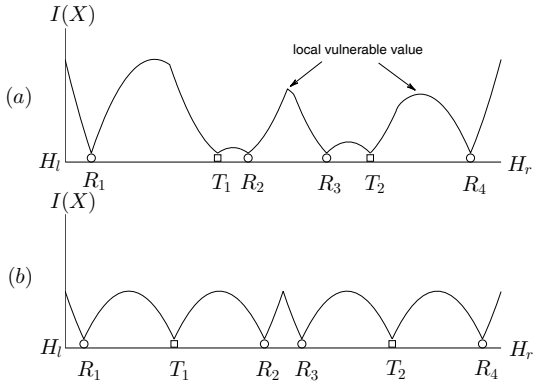

Figure 5: The local vulnerable values are (a) unequal with some placement spacing and (b) equal with balanced placement spacing.

An independent local order $\mathbf{S}_i$ has an *independent* property as described below. Note that the *closest* transmitter and *closest* receiver for any local vulnerable point on $Z_{\mathbf{S}_i}$ are nodes in $\mathbf{S}_i$. For example, for $\mathbf{S}_i = (T_1, R_1)$, the closest transmitter and closest receiver for $Y_{T_1R_1}$ are T_1 and R_1, respectively; for $\mathbf{S}_i = (T_1, R_1, \cdots, R_k, H_r)$, the closest transmitter for any of $Y_{T_1R_1}$, $\cdots$, $Y_{R_{k-1}R_k}$, and H_r, is T_1, while the closest receiver for any of $Y_{T_1R_1}$, $\cdots$, $Y_{R_{k-1}R_k}$, and H_r, is some node in $\{R_1, \cdots, R_k\}$. Therefore, *all the local vulnerable values on the independent local zone $Z_{\mathbf{S}_i}$, and hence the vulnerability $V(Z_{\mathbf{S}_i})$, are determined by the spacing $\mathbf{D}_{\mathbf{S}_i}$ (i.e., independent of any distance not in $\mathbf{D}_{\mathbf{S}_i}$).*

DEFINITION 8 (**Balanced Spacing**). *The spacing $\mathbf{D}_{\mathbf{S}}$ (or $\mathbf{D}_{\mathbf{S}_i}$) of an order $\mathbf{S}$ (or an independent local order $\mathbf{S}_i$, respectively) is balanced if all the local vulnerable values on $\overline{H_lH_r}$ (or the independent local zone $L_{\mathbf{S}_i}$, respectively) are equal (as illustrated in Figure 5).*

Using the independent property and Lemma 1, we can characterize the balanced spacing of an independent local order as follows.

LEMMA 2. *For any $c > 0$, let $e_c^0 \triangleq 2\sqrt{c}$ and e_c^j be the unique positive value of x such that $(\sum_{i=0}^{j-1} e_c^i + x/2)(x/2) = c$ for any $j \in \mathbb{N}^+$. For any $c > 0$ and any independent local order $\mathbf{S}_i$, there exists a unique balanced spacing $\mathbf{D}_{\mathbf{S}_i}$ such that $V(Z_{\mathbf{S}_i}) = c$. Furthermore, it is given by, e.g., for $\mathbf{S}_i = (T_1, R_1)$, $\mathbf{D}_{\mathbf{S}_i} = (e_c^0)$; for $\mathbf{S}_i = (T_1, R_1, \cdots, R_k, H_r)$,*

$$\mathbf{D}_{\mathbf{S}_i} = (e_c^0, e_c^1, \cdots, e_c^{k-1}, \frac{e_c^k}{2});$$

for $\mathbf{S}_i = (T_1, R_1, \cdots, R_k, T_2)$ and even k,

$$\mathbf{D}_{\mathbf{S}_i} = (e_c^0, e_c^1, \cdots, e_c^{\frac{k}{2}-1}, e_c^{\frac{k}{2}}, e_c^{\frac{k}{2}-1}, \cdots, e_c^1, e_c^0)$$

or odd k,

$$\mathbf{D}_{\mathbf{S}_i} = (e_c^0, e_c^1, \cdots, e_c^{\frac{k-1}{2}}, e_c^{\frac{k-1}{2}}, \cdots, e_c^1, e_c^0).$$

Similar results can be obtained for any other independent local order.

By definition, given c, the value of e_c^i, $i \in \mathbb{N}^+$ can be found iteratively and it decreases as i becomes larger (as shown in Table 1).

Table 1: Values of balanced spacing

c	e_c^0	e_c^1	e_c^2	e_c^3	e_c^4
1	2.0000	0.8284	0.6357	0.5359	0.4721
5	4.4721	1.8524	1.4214	1.1983	1.0557
10	6.3246	2.6197	2.0102	1.6947	1.4930
20	8.9443	3.7048	2.8428	2.3966	2.1115

Based on the independent property, we can cast a problem similar to problem (12) but for a *given* independent local order $\mathbf{S}_i$ as

$$\begin{aligned} \underset{\mathbf{D}_{\mathbf{S}_i}}{\text{maximize}} \quad & L_{\mathbf{S}_i} \\ \text{subject to} \quad & V(Z_{\mathbf{S}_i}) \le c. \end{aligned} \tag{13}$$

The balanced spacing proves to be the optimal spacing for problem (13).

LEMMA 3. *For any $c > 0$ and any independent local order $\mathbf{S}_i$, the balanced spacing $\mathbf{D}_{\mathbf{S}_i}$ such that $V(Z_{\mathbf{S}_i}) = c$ is the optimal spacing for problem* (13).

Next we turn to show that the optimal order has a *dividable* structure.

DEFINITION 9 (**Dividable Order**). *An order $\mathbf{S}$ is dividable if it consists of independent local orders $\mathbf{S}_1, \cdots, \mathbf{S}_m$ such that 1) each node in $\mathbf{S}$ is included in some $\mathbf{S}_i$; 2) the last node of $\mathbf{S}_i$ is the first node of $\mathbf{S}_{i+1}$ for all $i = 1, \cdots, m-1$. Therefore, $\overline{H_lH_r}$ under $\mathbf{S}$ consists of independent local zones $Z_{\mathbf{S}_1}$, $\cdots$, $Z_{\mathbf{S}_m}$, and $\mathbf{D}_{\mathbf{S}}$ consists of disjoint sets of spacing distances $\mathbf{D}_{\mathbf{S}_1}$, $\cdots$, $\mathbf{D}_{\mathbf{S}_m}$.*

For example,

$$\mathbf{S} = (\overbrace{H_l, R_1, R_2, \underbrace{T_1}_{\mathbf{S}_2}}^{\mathbf{S}_1}, R_3, R_4, R_5, \overbrace{\underbrace{T_2}_{\mathbf{S}_2}, \underbrace{R_6}_{\mathbf{S}_4}}^{\mathbf{S}_3}, T_3, T_4, H_r) \tag{14}$$

is a dividable order.

LEMMA 4. *The optimal order $\mathbf{S}^*$ is dividable.*

It is worth mentioning that Lemma 4 provides a *necessary* condition for the optimal order. In other words, a non-optimal order (such as (14)) can also have this structure.

The structure of a dividable order allows us to break down the problem. Consider the following problem that is related to problem (12) but for a *given* order $\mathbf{S}$:

$$\begin{aligned} \underset{\mathbf{D}_{\mathbf{S}}}{\text{maximize}} \quad & \|H_lH_r\| \\ \text{subject to} \quad & V(\overline{H_lH_r}) \le c. \end{aligned} \tag{15}$$

For a dividable order $\mathbf{S}$, the set of local vulnerable points on $\overline{H_lH_r}$ is the union of *disjoint* sets of local vulnerable points on the independent local zones $Z_{\mathbf{S}_1}$, $\cdots$, $Z_{\mathbf{S}_m}$ of independent local orders $\mathbf{S}_1, \cdots, \mathbf{S}_m$. Therefore, *problem* (15) *for a dividable order $\mathbf{S}$ can be broken down into independent subproblems, each of which is an instance of problem* (13) *for one of $\mathbf{S}_1, \cdots, \mathbf{S}_m$*, such that each can be solved using Lemma 3. Note that if the optimal order $\mathbf{S}^*$ is known, then problem (12) boils down to problem (15) for $\mathbf{S} = \mathbf{S}^*$. Since the optimal order $\mathbf{S}^*$ is dividable by Lemma 4, the next result directly follows.

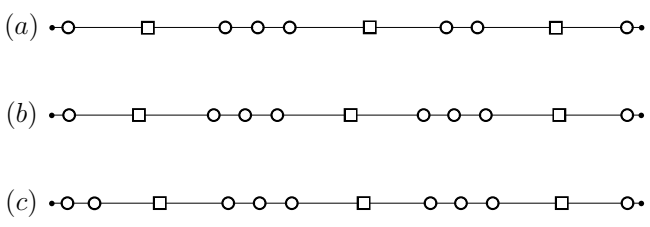

Figure 6: Optimal placement of transmitters (square) and receivers (circle) for (a) $M = 3$, $N = 7$; (b) $M = 3$, $N = 8$; (c) $M = 3$, $N = 9$.

THEOREM 2. *For the optimal order $\mathbf{S}^*$ and any $c > 0$, the balanced spacing $\mathbf{D}_{\mathbf{S}^*}$ such that $V(\overline{H_l H_r}) = c$ exists and is the optimal spacing for problem (15) for $\mathbf{S} = \mathbf{S}^*$.*

Next we characterize the optimal order $\mathbf{S}^*$. Let $f_c^{\mathbf{S}}$ denote the optimal value of problem (15) for an order $\mathbf{S}$ under the constraint $V(\overline{H_l H_r}) \leq c$. Then $f_c^{\mathbf{S}}$ achieves the maximum when $\mathbf{S} = \mathbf{S}^*$. Since all transmitters are homogeneous, we index the transmitters from left to right such that $0 \leq \|H_l T_1\| \leq \cdots \leq \|H_l T_M\| \leq \|H_l H_r\|$. Define

$$\mathbf{N_S} \triangleq (n_1, n_2, \cdots, n_M, n_{M+1})$$

where n_i, n_1, n_{M+1} denote the number of receivers in $\mathbf{S}$ between T_{i-1} and T_i for $i \in \{2, \cdots, M\}$, between H_l and T_1, between T_M and H_r, respectively. Since all receivers are homogeneous, it suffices to determine $\mathbf{N}_{\mathbf{S}^*}$ for characterizing the optimal order $\mathbf{S}^*$.

THEOREM 3. *An order $\mathbf{S}$ is optimal if and only if*

$$|n_i - n_j| \leq 1, \forall i, j \in \{2, \cdots, M\}$$
$$|n_i - 2n_1| \leq 1, |n_i - 2n_{M+1}| \leq 1, \forall i \in \{2, \cdots, M\}.$$

Using Theorem 3, we can describe the optimal order $\mathbf{S}^*$ as follows. Let two integers q and r be the quotient and remainder of N/M, respectively. If q is even, we have

$$\mathbf{N}_{\mathbf{S}^*} = (\frac{q}{2}, \overbrace{q+1, \cdots, q+1}^{r}, \overbrace{q, \cdots, q}^{M-1-r}, \frac{q}{2});$$

if q is odd and $r = 0$, we have

$$\mathbf{N}_{\mathbf{S}^*} = (\frac{q+1}{2}, \overbrace{q, \cdots, q}^{M-1}, \frac{q-1}{2});$$

if q is odd and $r \geq 1$, we have

$$\mathbf{N}_{\mathbf{S}^*} = (\frac{q+1}{2}, \overbrace{q+1, \cdots, q+1}^{r-1}, \overbrace{q, \cdots, q}^{M-r}, \frac{q+1}{2}).$$

In addition, any order obtained from the above optimal order by swapping the values of n_1 and n_{M+1}, or the values of n_i and n_j for $i, j \in \{2, \cdots, M\}$, also satisfies the conditions in Theorem 3, and hence is optimal.

Given the optimal order $\mathbf{S}^*$ for problem (12), we can find the optimal spacing $\mathbf{D}^*_{\mathbf{S}^*}$ for problem (12) by using Theorem 2 to solve problem (15) for $\mathbf{S}^*$.

4.3 Discussions

The optimal order and the optimal spacing both present elegant *balanced* structures (as illustrated in Figure 6). As noted earlier, the optimal spacing is balanced in the sense that all the local vulnerable values on $\overline{H_l H_r}$ are *equal* under the optimal spacing. The optimal orders are balanced in a more subtle sense: for the optimal order $\mathbf{S}^*$, n_i is *as equal as possible* across all $i = 2, \cdots, M$, and it is *as equal as possible to twice* the value of n_1, n_{M+1}, respectively. The balanced structures are partly due to that all the BRs are homogeneous.

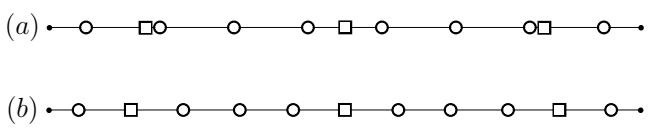

Figure 7: Heuristic placement of transmitters (square) and receivers (circle) for $M = 3$, $N = 8$: (a) HEU-1; (b) HEU-2.

The optimal placement results imply that one assumption made in Section 2 can be greatly relaxed without losing the optimality. Since the detectability of a point is determined by the closest transmitter and closest receiver, it suffices for a receiver to pair with a transmitter only if they are the closest receiver and closest transmitter, respectively, for some point on the line barrier. Thus, under the optimal placement of a BRN consisting of more receivers than transmitters (such as in Figure 6), one can see that a receiver only needs to pair with its closest transmitter(s), the number of which is *one or two*.

5. NUMERICAL RESULTS

In this section, we present numerical results to illustrate the effectiveness of the optimal placement of BRs on a line barrier H.

As none of the existing works has studied the placement of BRs for barrier coverage, we compare the optimal placement strategy (OPT) with two heuristic strategies. The heuristics are motivated by the rationale of the optimal placement strategy for a network of homogeneous sensors under the disk sensing model, which is to minimize the maximum distance from a point on H to its closest sensor.

One heuristic (HEU-1) is to place transmitters (or receivers, respectively) with uniform spacing such that the maximum distance from a point on H to its closest transmitter (or receiver, respectively) is minimized (as illustrated in Figure 7(a)):

$$2\|H_l T_1\| = \|T_1 T_2\| = \cdots = \|T_{M-1} T_M\| = 2\|T_M H_r\|$$

$$2\|H_l R_1\| = \|R_1 R_2\| = \cdots = \|R_{N-1} R_N\| = 2\|R_N H_r\|.$$

We can see from Figure 6 that neither the transmitters nor the receivers in OPT follow the placement of HEU-1. Compared to OPT, the drawback of HEU-1 is mainly due to that it places transmitters and receivers *independently*.

Another heuristic (HEU-2) is to place transmitters and receivers according to the optimal order $\mathbf{S}^*$, but with uniform spacing such that the maximum distance from a point on H to its closest BR node (transmitter or receiver) is minimized (as illustrated in Figure 7(b)):

$$2\|H_l S_1\| = \|S_1 S_2\| = \cdots = \|S_{M-1} S_M\| = 2\|S_M H_r\|.$$

Although HEU-2 follows the optimal order, its main drawback lies in that it treats transmitters and receivers *equivalently*.

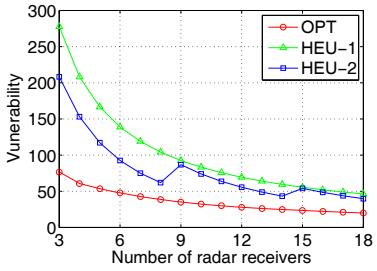

Figure 8: Vulnerability for 3 transmitters.

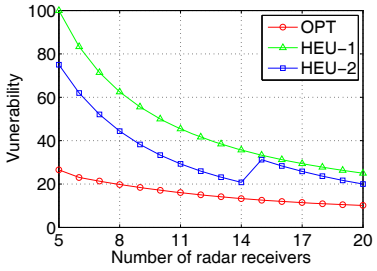

Figure 9: Vulnerability for 5 transmitters.

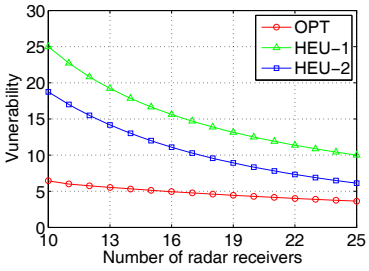

Figure 10: Vulnerability for 10 transmitters.

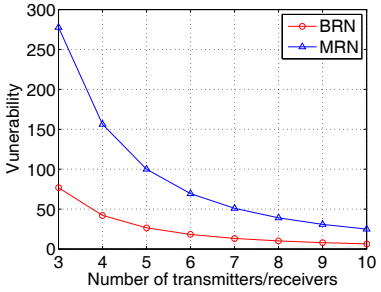

Figure 11: Minimum vulnerability: BRN vs MRN.

Figure 8, Figure 9 and Figure 10 depict the vulnerability of H under OPT, HEU-1, and HEU-2 for a varying number of receivers and 3, 5, 10 transmitters, respectively. We set the length of H to 100m. We observe that HEU-2 results in considerably lower vulnerability than HEU-1, and OPT further outperforms HEU-2 significantly. This shows that OPT is highly advantageous for improving the barrier coverage, which is essentially due to that the design rationale for a BRN under the Cassini oval sensing model is quite different and more complicated than that for a network of passive sensors (or MRs) under the disk sensing model. Therefore, the optimal placement of a BRN requires judicious design of transmitters and receivers as we do in this paper.

In Figure 11, we compare the vulnerability of H under the optimal placement of a BRN to that of a monostatic radar network (MRN) for a varying number of transmitters and receivers. The optimal placement strategy for a MRN is to minimize the maximum distance from a point on H to its closest MR. For fair comparison, we set the number of transmitters equal to that of receivers in the BRN, and also equal to the number of MRs in the MRN. We observe that the advantage of a BRN is significant, which demonstrates that the flexibility to place transmitters and receivers separately is highly beneficial for barrier coverage.

6. RELATED WORK

Radar has been extensively studied for decades [12]. However, radar sensor networks have garnered attention only in the past few years, largely driven by the emergence of cheaper and more compact radar sensors replacing conventionally expensive and bulky radar systems. For example, in [13], a platform has been successfully designed and built to integrate ultrawideband radars with mote-class sensor devices. The existing literature has studied different problems for radar sensor networks, including waveform design and diversity [14], radar scheduling [15], data management [16], for a variety of objectives, such as target detection [17] and localization [18]. In particular, BRs have also been considered in [18]. However, coverage problems of a radar sensor network have received very little attention. Recently, a novel Doppler coverage model has been introduced in [19] for a radar sensor network that exploits the Doppler effect. To our best knowledge, our work is the first to explore the coverage of a network of BRs.

Numerous studies on sensor network coverage can be found in the literature [7]. Worst-case intrusion was first introduced in [9]. [9, 10, 20] have studied how to find the worst-case intrusion path for arbitrary deployed sensors. [21, 22] have considered adding sensors to improve the coverage of the worst-case intrusion path. Along another avenue, barrier coverage was first introduced in [3] and has attracted much research interests recently. [3,5] have studied the critical sensor density for barrier coverage under random deployment. The coverage of a barrier has been investigated using a quantitative metric in [4]. Barrier coverage of sensors with mobility have been considered in [6, 23]. Barrier coverage for camera sensor networks has also been studied recently based on a novel full-view coverage model [24, 25].

While most aforementioned studies are concerned with how to find the worst-case intrusion path or a barrier covered by sensors (if such a barrier exists) under an *existing* deployment of sensors, this work focuses on *where* we should deploy sensors to cover a barrier such that the worst-case intrusion detectability is maximized. More importantly, the existing sensing models (particularly the widely used disk sensing model) are quite different from the Cassini oval sensing model of a BR, and the latter is further complicated by the coupling of sensing regions across multiple BRs.

7. CONCLUSION AND FUTURE WORK

Radar sensor networks have great potential in many applications, such as border surveillance and traffic monitoring. In this paper, we studied the problem of deploying a BRN for barrier coverage. The optimal placement of BRs is highly non-trivial, since 1) the coverage region of a BR is characterized by a Cassini oval that presents complex geometry; 2) the coverage regions of different BRs are coupled and the network coverage is intimately related to the locations of all BR nodes. We show that it is in general not optimal to place the BRs on the shortest barrier, but it is optimal if the shortest barrier is also the shortcut barrier. Further,

we characterized the optimal placement order and the optimal placement spacing of the BRs on a line barrier, both of which present elegant balanced structures.

Although the models are built upon some idealized assumptions, we believe that this work provides some initial steps for understanding the coverage of networked BRs. There are still many questions remaining open. For example, while the Cassini oval sensing model used in this work is based on SNR, it would be interesting to also take into account the *Doppler effect*. As the Doppler effect is intimately related to the motion of objects, it would give rise to a number of challenging problems in the context of networked radars. Furthermore, as this work assumes that all BRs are homogeneous, an interesting future direction is to consider a network of heterogeneous BRs.

ACKNOWLEDGEMENT

This research was supported in part by the NSF Grant CNS-0901451, U.S. AFOSR project FA9550-10-1-0464, DoD MURI project No. FA9550-09-1-0643, and NSFC Grant 61170267.

8. REFERENCES

[1] C. J. Baker and H. D. Griffiths, "Bistatic and multistatic radar sensors for homeland security," *Advances in Sensing with Security Applications*, vol. 2, pp. 1–22, Feb. 2006.

[2] B. Donovan, D. J. McLaughlin, and J. Kurose, "Principles and design considerations for short-range energy balanced radar networks," in *IGARSS 2005*.

[3] S. Kumar, T.-H. Lai, and A. Arora, "Barrier coverage with wireless sensors," in *ACM MOBICOM 2005*.

[4] A. Chen, T.-H. Lai, and D. Xuan, "Measuring and guaranteeing quality of barrier-coverage in wireless sensor networks," in *ACM MOBIHOC 2008*.

[5] B. Liu, O. Dousse, J. Wang, and A. Saipulla, "Strong barrier coverage of wireless sensor networks," in *ACM MOBIHOC 2008*.

[6] A. Saipulla, B. Liu, G. Xing, X. Fu, and J. Wang, "Barrier coverage with sensors of limited mobility," in *ACM MOBIHOC 2010*.

[7] B. Wang, "Coverage problems in sensor networks: A survey," *ACM Computing Surveys*, vol. 43, Oct. 2011.

[8] N. Willis, *Bistatic Radar*. SciTech Publishing, 2005.

[9] S. Meguerdichian, F. Koushanfar, M. Potkonjak, and M. Srivastava, "Coverage problems in wireless ad-hoc sensor network," in *IEEE INFOCOM 2001*.

[10] S. Meguerdichian, S. Slijepcevic, V. Karayan, and M. Potkonjak, "Localized algorithms in wireless ad-hoc networks: Location discovery and sensor exposure," in *ACM MOBIHOC 2001*.

[11] X.-Y. Li, P.-J. Wan, and O. Frieder, "Coverage in wireless ad hoc sensor networks," *IEEE Transactions on Computers*, vol. 52, pp. 753–763, Jun. 2003.

[12] M. Skolnik, *Introduction to radar systems*. McGraw-Hill, 2002.

[13] A. A. Dutta, P. and S. Bibyk, "Towards radar-enabled sensor networks," in *ACM/IEEE IPSN 2006*.

[14] Q. Liang, "Waveform design and diversity in radar sensor networks: Theoretical analysis and application to automatic target recognition," in *IEEE SECON 2006*.

[15] T. Hanselmann, M. Morelande, B. Moran, and P. Sarunic, "Constrained multi-object Markov decision scheduling with application to radar resource management," in *Infomation Fusion 2010*.

[16] M. Li, T. Yan, D. Ganesan, E. Lyons, P. Shenoy, A. Venkataramani, and M. Zink, "Multi-user data sharing in radar sensor networks," in *ACM SenSys 2007*.

[17] S. Bartoletti, S. Conti, and A. Giorgetti, "Analysis of UWB radar sensor networks," in *IEEE ICC 2010*.

[18] E. Paolini, A. Giorgetti, M. Chiani, R. Minutolo, and M. Montanari, "Localization capability of cooperative anti-intruder radar systems," *EURASIP Journal on Advances in Signal Processing*, 2008.

[19] X. Gong, J. Zhang, and D. Cochran, "When target motion matters: Doppler coverage in radar sensor networks," in *IEEE INFOCOM 2013*.

[20] S. Meguerdichian, F. Koushanfar, G. Qu, and M. Potkonjak, "Exposure in wireless ad-hoc sensor network," in *ACM MOBICOM 2001*.

[21] R.-H. Gau and Y.-Y. Peng, "A dual approach for the worst-case-coverage deployment problem in ad-hoc wireless sensor networks," in *IEEE MASS 2006*.

[22] C. Lee, D. Shin, S.-W. Bae, and S. Choi, "Best and worst-case coverage problems for arbitrary paths in wireless sensor networks," in *IEEE MASS 2010*.

[23] G.-Y. Keung, B. Li, and Q. Zhang, "The intrusion detection in mobile sensor network," in *ACM MOBIHOC 2010*.

[24] Y. Wang and G. Cao, "Barrier coverage in camera sensor networks," in *ACM MOBIHOC 2011*.

[25] H. Ma, Y. Meng, D. Li, Y. Hong, and W. Chen, "Minimum camera barrier coverage in wireless camera sensor networks," in *IEEE INFOCOM 2012*.

[26] X. Gong, J. Zhang, and D. Cochran, "Optimal placement for barrier coverage in bistatic radar sensor networks," Tech. Rep., http://informationnet.asu.edu/bistatic-radar.pdf.

APPENDIX

In this section, due to space limitation, we only provide the main ideas of the proofs of the results presented in this paper. The detailed proofs can be found in our online technical report [26].

PROOF SKETCH OF THEOREM 1

For any barrier $\widetilde{AB}$ and the optimal placement $\{T_i, R_j\}$ for minimizing $V(\widetilde{AB})$, we can construct a placement $\{T_i', R_j'\}$ for $\overline{AB}$ by moving each T_i (or R_j) to its projection T_i' (or R_j', respectively) on the line passing through A and B (not necessarily falls on $\overline{AB}$), as illustrated in Figure 12(a). Then for any point $X' \in \overline{AB}$, there exists a point $X \in \widetilde{AB}$ whose projection on $\overline{AB}$ is X', and we can show that $I'(X')^8 \leq I(X)$. This implies that $V(\overline{AB})$ under $\{T_i', R_j'\}$ is no greater than $V^*(\widetilde{AB})$, and hence $V^*(\overline{AB}) \leq V^*(\widetilde{AB})$. Since $V^*(U)$ for a

[8]We will use $I'(X)$ and $I^-(X)$ to denote the detectability of a point X under a placement of nodes with superscripts $'$ and $^-$, respectively.

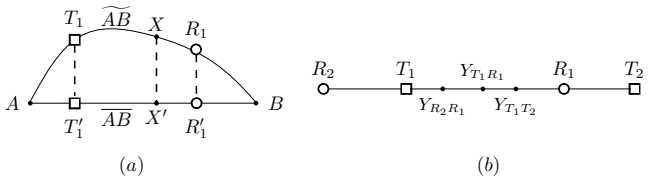

Figure 12: Examples of proofs of (a) Theorem 1 and (b) Lemma 1.

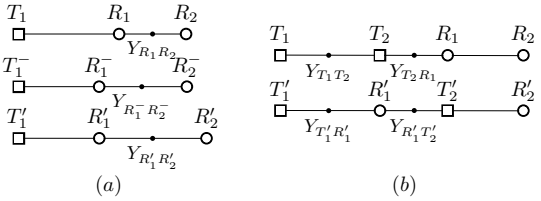

Figure 13: Examples of proofs of (a) Lemma 3 and (b) Lemma 4.

line barrier U is increasing with U's length and the shortcut barrier H is no longer than $\overline{AB}$, we have $V^*(H) \leq V^*(\overline{AB}) \leq V^*(\widetilde{AB})$.

PROOF SKETCH OF LEMMA 1

The main idea of this proof is to divide the line segment between each pair of neighbor nodes into intervals such that all points on an interval have the *same* closest BR, and then we examine the detectability structure on each interval. For example, suppose T_1 and R_1 are neighbor nodes as illustrated in Figure 12(b). Then suppose there exist $R_2 \in \overline{H_lT_1}$ and $T_2 \in \overline{R_1H_r}$ such that the closest BRs for a point on $\overline{T_1Y_{R_2R_1}}$, $\overline{Y_{R_2R_1}Y_{T_1T_2}}$, $\overline{Y_{T_1T_2}R_1}$ are $T_1 - R_2$, $T_1 - R_1$, $T_2 - R_1$, respectively. We can show that $I(X)$ increases as $X \in \overline{T_1Y_{R_2R_1}}$ is closer to $Y_{R_2R_1}$; $I(X)$ increases as $X \in \overline{Y_{R_2R_1}Y_{T_1T_2}}$ is closer to $Y_{T_1R_1}$; $I(X)$ decreases as $X \in \overline{Y_{T_1T_2}R_1}$ is closer to R_1. Therefore, $I(X)$ attains maximum on $\overline{T_1R_1}$ when $X = Y_{T_1R_1}$.

PROOF SKETCH OF LEMMA 2

The main idea of this proof is to successively determine the distances between neighbor nodes. For example, suppose $\mathbf{S}_i = (T_1, R_1, \cdots, R_k, H_r)$ and $\mathbf{D}_{\mathbf{S}_i}$ is balanced such that $V(\overline{T_1H_r}) = c$. Since $I(Y_{T_1R_1}) = (\|T_1R_1\|/2)^2 = c$, we obtain $\|T_1R_1\| = 2\sqrt{c} = e_c^0$. Then since $I(Y_{R_1R_2}) = \|T_1Y_{R_1R_2}\|$ $\|Y_{R_1R_2}R_2\| = (\|T_1R_1\| + \|R_1R_2\|/2)$ $(\|R_1R_2\|/2) = c$, using $\|T_1R_1\| = 2\sqrt{c}$, we obtain a unique value e_c^1 for $\|R_1R_2\|$. Following the same argument recursively, using the values of $\|T_1R_1\|$, $\cdots$, $\|R_{i-1}R_i\|$, we obtain a unique value e_c^i for $\|R_iR_{i+1}\|$ such that $I(Y_{R_iR_{i+1}}) = c$ ... until we obtain a unique value $e_c^k/2$ for $\|R_kH_r\|$ such that $I(H_r) = c$.

PROOF SKETCH OF LEMMA 3

The proof is based on contradiction. For example, suppose $\mathbf{S}_i = (T_1, R_1, \cdots, R_k, H_r)$ with balanced spacing $\mathbf{D}_{\mathbf{S}_i}$ such that $V(Z_{\mathbf{S}_i}) = c$. Suppose there exists another placement $\mathbf{S}_i' = (T_1', R_1', \cdots, R_k', H_r')$ with spacing $\mathbf{D}_{\mathbf{S}_i'}$ such that $V(Z_{\mathbf{S}_i'}) \leq c$ and $\|T_1'H_r'\| > \|T_1H_r\|$. Since $I(Y_{T_1R_1}) = (\|T_1R_1\|/2)^2 \geq I'(Y_{T_1'R_1'}) = (\|T_1'R_1'\|/2)^2$, we have $\|T_1'R_1'\| \leq \|T_1R_1\|$. Then, using this and $I(Y_{R_1R_2}) \geq I'(Y_{R_1'R_2'})$, we can show that $\|T_1'R_2'\| \leq \|T_1R_2\|$: As illustrated in Figure 13(a), if $\|T_1'R_2'\| > \|T_1R_2\|$, we can find $\{T_1^-, R_1^-, R_2^-\}$ with $\|T_1^-R_1^-\| = \|T_1'R_1'\|$ and $\|T_1^-R_2^-\| = \|T_1R_2\|$ such that $I'(Y_{R_1'R_2'}) > I^-(Y_{R_1^-R_2^-}) > I(Y_{R_1R_2})$, which is a contradiction. Following the same argument recursively, using $\|T_1'R_{i-1}'\| \leq \|T_1R_{i-1}\|$ and $I(Y_{R_{i-1}R_i}) \geq I'(Y_{R_{i-1}'R_i'})$, we can show that $\|T_1'R_i'\| \leq \|T_1R_i\|$ ... until we can show that $\|T_1'H_r'\| \leq \|T_1H_r\|$, which is a contradiction.

PROOF SKETCH OF LEMMA 4

The proof is based on the following result: The optimal order does not have a local order with one of these node types: (T, T, R, R), (R, R, T, T), (H_l, R, T, T), (H_l, T, R, R), (R, R, T, H_r), (T, T, R, H_r). We can use a *swapping* argument to show this result. For example, suppose $\mathbf{S} = (\cdots, T_1, T_2, R_1, R_2, \cdots)$ with any spacing $\mathbf{D}_\mathbf{S}$. We can construct a new order $\mathbf{S}' = (\cdots, T_1', R_1', T_2', R_2', \cdots)$ from $\mathbf{S}$ with the same *values* of spacing $\mathbf{D}_{\mathbf{S}'}$ by swapping the *locations* of nodes T_2 and R_1. Then we can show that any local vulnerable value (and hence the vulnerability) under $\mathbf{S}'$ and $\mathbf{D}_{\mathbf{S}'}$ must be *no greater than* that under $\mathbf{S}$ and $\mathbf{D}_\mathbf{S}$. For example, as illustrated in Figure 13(b), since the closest BRs to $Y_{T_2R_1}$, $Y_{R_1'T_2'}$ are $T_2 - R_1$, $T_2' - R_1'$, respectively, we have $I(Y_{T_2R_1}) = I'(Y_{R_1'T_2'})$; since the closest transmitters to $Y_{T_1T_2}$, $Y_{T_1'R_1'}$ are T_1, T_1', respectively, and the distance from $Y_{T_1T_2}$ to $Y_{T_1T_2}$'s closest receiver is no less than that from $Y_{T_1'R_1'}$ to $Y_{T_1'R_1'}$'s closest receiver, we have $I(Y_{T_1T_2}) \geq I'(Y_{T_1'R_1'})$. This implies that $\mathbf{S}$ is not the optimal order.

Based on the above result, we next show that the optimal order $\mathbf{S}^*$ must be dividable. We construct a *super order* $\mathbf{S}^+$ from an order $\mathbf{S}$ by combining neighbor nodes of the same type in $\mathbf{S}$ into a *super node*. For the example in (14), the super order is given by $\mathbf{S}^+ = (H_l, R_{1,2}^+, T_1, R_{3,4,5}^+, T_2, R_6, T_{3,4}^+, H_r)$. By construction, two neighbor nodes in $\mathbf{S}^+$ (excluding H_l and H_r) are of different types (transmitter or receiver type). Using the previous result, for $\mathbf{S}^+$ constructed from the optimal order $\mathbf{S}^*$, two neighbor nodes in $\mathbf{S}^+$ cannot be both super nodes, and a super node cannot be the third or third-to-last node in $\mathbf{S}^+$. Then we can see that $\mathbf{S}^*$ must have the dividable structure.

PROOF SKETCH OF THEOREM 3

We first can show that the optimal order $\mathbf{S}^*$ must have $n_i \geq 1$ for all $i \in \{1, \cdots, M+1\}$. Based on this, we can see that $\mathbf{S}^*$ consists of independent local orders $(H_l, \cdots, T_1)$, $\cdots$, $(T_{i-1}, \cdots, T_i)$, $\cdots$, $(T_M, \cdots, H_r)$. Let $g_c(n)$ denote the optimal value of problem (13) for such an independent local order $(T_{i-1}, \cdots, T_i)$ containing n receivers under the constraint $V(Z_{\mathbf{S}_i}) \leq c$. Then we have $f_c^{\mathbf{S}^*} = \sum_{i=2}^{M} g_c(n_i) + g_c(2n_1)/2 + g_c(2n_{M+1})/2$. By Lemma 2 and Lemma 3, we have $g_c(n) = 2\sum_{i=0}^{\frac{n}{2}-1} e_c^i + e_c^{\frac{n}{2}}$ if n is even or $2\sum_{i=0}^{\frac{n+1}{2}-1} e_c^i$ if n is odd. Then it follows that $g_c(n+1) - g_c(n) = e_c^{\frac{n}{2}}$ if n is even or $e_c^{\frac{n+1}{2}}$ if n is odd, and $g_c(2n+2) - g_c(2n) = e_c^{n+1} + e_c^n$. Using these, we can show that if $\mathbf{S}^*$ does not satisfy the desired conditions, there exists some $\mathbf{S}'$ constructed from $\mathbf{S}^*$ by adding n_i by 1 while subtracting n_j by 1 for some $i \neq j$ such that $f_c^{\mathbf{S}^*} < f_c^{\mathbf{S}'}$, which contradicts that $\mathbf{S}^*$ is optimal.